

Generating Multiparticle Entangled States by Self-Organization of Driven Ultracold Atoms

Ivor Krešić^{1,2,*}, Gordon R. M. Robb³, Gian-Luca Oppo,³ and Thorsten Ackemann³

¹Institute for Theoretical Physics, Vienna University of Technology (TU Wien), Vienna, A-1040, Austria

²Centre for Advanced Laser Techniques, Institute of Physics, Bijenička cesta 46, 10000, Zagreb, Croatia

³SUPA and Department of Physics, University of Strathclyde, Glasgow G4 0NG, Scotland, United Kingdom



(Received 19 August 2022; accepted 7 September 2023; published 18 October 2023)

We describe a mechanism for guiding the dynamical evolution of ultracold atomic motional degrees of freedom toward multiparticle entangled Dicke-squeezed states, via nonlinear self-organization under external driving. Two examples of many-body models are investigated. In the first model, the external drive is a temporally oscillating magnetic field leading to self-organization by interatomic scattering. In the second model, the drive is a pump laser leading to transverse self-organization by photon-atom scattering in a ring cavity. We numerically demonstrate the generation of multiparticle entangled states of atomic motion and discuss prospective experimental realizations of the models. For the cavity case, the calculations with adiabatically eliminated photonic sidebands show significant momentum entanglement generation can occur even in the “bad cavity” regime. The results highlight the potential for using self-organization of atomic motion in quantum technological applications.

DOI: 10.1103/PhysRevLett.131.163602

The study of self-organization of ultracold atoms is a well-established research direction, with many notable experimental and theoretical results [1,2]. Following the pioneering works on self-organization of cold [3,4] and ultracold [5,6] atoms coupled to a single longitudinal mode of a Fabry-Perot cavity, the multimode aspects of optomechanical self-organization in cold and ultracold atoms have recently started to generate significant interest [7–26]. In parallel to the work on optomechanical self-organization, there has been great progress in studying the atomic self-organization arising due to atom-atom interactions being modulated by an external B -field [27–31].

Although the majority of these works have studied the nonequilibrium phase diagrams in the mean field limit, where quantum correlations can be neglected, a number of works have shown that the quantum nature of light and matter can play an important role for self-organization [6,32–41].

Quantum correlated squeezed and entangled states can be used for quantum enhanced measurements, which go beyond classical metrology [42,43]. In this context, squeezing and entanglement of the internal atomic degrees of freedom [44–55], but recently also the external ones [56–60], have been recognized as attractive tools for metrological applications.

Here, we focus on external degrees of freedom and study the spontaneous generation of multiparticle entangled (also called Dicke-squeezed) states in the atomic motion [53,61–66] by self-organization of an externally driven Bose-Einstein condensate (BEC). The mechanism of this phenomenon is four-wave mixing [67–73] of zero-order

modes with the spontaneously generated transverse sidebands, and we demonstrate the effect numerically for two different models. In the first model, the self-organization arises due to an external periodic modulation in interatomic scattering driven by a temporally oscillating B -field. In the second model, it arises from laser driving in a ring cavity. A confinement along the y and z axes allows us to restrict the analysis to 1D structures in an elongated cloud.

Driving by B -field modulation.—In the first model, shown in Fig. 1(a), a spatially homogeneous and temporally oscillating B -field in the z direction is modulated near a Feshbach resonance of the atoms. The B -field sinusoidally modulates the atomic s -wave scattering length with frequency ω_{mod} and amplitude a_{mod} , thus driving the pattern formation [31]. For a collisionally thin medium, this four-wave mixing process is described by the three-mode Hamiltonian:

$$H_B = i\hbar g_{\text{mod}} b_+^\dagger b_-^\dagger b_0 b_0 + \text{H.c.}, \quad (1)$$

where $g_{\text{mod}} = 2\pi\hbar a_{\text{mod}}/mV$, m is the atom mass, V is the volume of the condensate, and b_0 , b_\pm are the bosonic momentum annihilation operators for the transverse modes of momenta 0, $\pm\hbar k_f$, where $k_f = \sqrt{m\omega_{\text{mod}}/\hbar}$. The mechanism of pattern formation in this system is illustrated in Fig. 1(b). When a pair of atoms with zero transverse momenta absorbs a quantum of energy $\hbar\omega_{\text{mod}}$, they scatter into modes with opposite momenta and kinetic energies $\hbar\omega_{\text{mod}}/2$. This momentum-conserving process leads in the

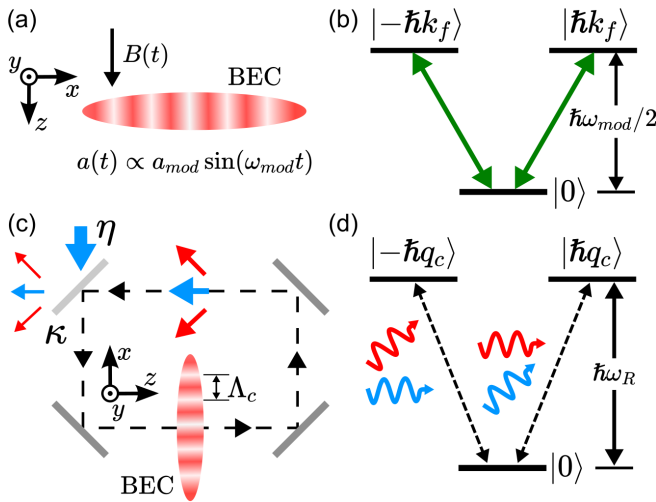


FIG. 1. Nonlinear self-organization via four-wave mixing of momentum modes in a driven BEC. (a) The self-organization along the x axis can be driven by applying a B -field $B(t)$ oscillating near a Feshbach resonance, leading to an oscillating scattering length $a(t)$ [31]. (b) Absorption of a quantum of energy $\hbar\omega_{\text{mod}}$ leads here to a momentum-conserving scattering of two atoms with zero transverse momentum into modes with transverse momenta $\pm\hbar k_f$, where $k_f = \sqrt{m\omega_{\text{mod}}/\hbar}$. (c) Transverse self-organization with spatial period Λ_c for laser pumped atoms in a ring cavity (η pump rate) with photon leakage rate κ . (d) In this system, an atomic sideband with transverse momentum $-\hbar q_c$ ($q_c = 2\pi/\Lambda_c$) is excited by scattering of an on-axis photon into a vacuum mode with transverse wave number $+q_c$. A correlated atom with transverse momentum $+\hbar q_c$ can then be created if this sideband photon is scattered back into the on-axis mode, with a converse process for the $-q_c$ photon sideband (not shown).

semiclassical picture to a formation of stripe patterns in the atomic density.

Note that the Hamiltonian H_B describes the same physics for atoms as the two-photon formalism of [74–77] does for photon pairs generated in optical parametric amplifiers. Moreover, H_B is the atomic momentum equivalent of the Hamiltonian used in SU(1,1) spin-1 atom interferometry [78,79].

Laser driving with ring cavity feedback.—The second model we study is based on laser driving of a BEC in a ring cavity, as illustrated in Fig. 1(c). This novel setup is inspired by earlier theoretical proposals [32–34,80–82]. Such transverse self-organization has been observed in nearly degenerate Fabry-Perot cavity experiments with vertical-cavity regenerative amplifiers [83] and photorefractive crystals [84,85]. For a BEC in a cavity, in addition to the three atomic motional modes with annihilation operators b_0 , b_{\pm} for transverse momenta 0, $\pm\hbar q_c$ (with $q_c = 2\pi/\Lambda_c$ for the pattern length scale Λ_c), we have also the corresponding intracavity photonic modes with annihilation operators a_0 , a_{\pm} . In this system, a continuous-wave laser of frequency ω drives the zero-order cavity mode of frequency ω_0 with pump rate η . Above some critical pump

level η_c , this leads to spontaneous generation of sideband modes with frequency ω'_0 , concurrently with atomic momentum sideband modes. The effective Hamiltonian of the problem is given by $H_{\text{cav}} = H_0 + H_{\text{FWM}}^{(1)} + H_{\text{FWM}}^{(2)}$, with

$$H_0 = -\hbar\bar{\Delta}_c n_0 - \hbar\bar{\Delta}'_c(n_+ + n_-) + \hbar\omega_R(N_+ + N_-) + i\hbar\eta(a_0^\dagger - a_0), \quad (2)$$

and the four-wave mixing terms

$$H_{\text{FWM}}^{(1)} = \hbar U_0[(a_+^\dagger b_-^\dagger + a_-^\dagger b_+^\dagger)a_0 b_0 + \text{H.c.}] + \hbar U_0[a_0^\dagger(b_+^\dagger a_+ + b_-^\dagger a_-)b_0 + \text{H.c.}], \quad (3)$$

$$H_{\text{FWM}}^{(2)} = \hbar U_0(a_+^\dagger a_- b_-^\dagger b_+ + \text{H.c.}), \quad (4)$$

where $\bar{\Delta}_c = \omega - \omega_0 - NU_0$, $\bar{\Delta}'_c = \omega - \omega'_0 - NU_0$ are the effective pump detunings from the on-axis and sideband cavity modes, respectively, $n_0 = a_0^\dagger a_0$, $n_{\pm} = a_{\pm}^\dagger a_{\pm}$, $N_0 = b_0^\dagger b_0$, $N_{\pm} = b_{\pm}^\dagger b_{\pm}$, $U_0 = g_0^2/\Delta_a$ is the single atom light shift, $\Delta_a = \omega - \omega_a$ is the laser-atom detuning of the two-level optical transition, g_0 is the atom-cavity coupling strength, and $\hbar\omega_R = (\hbar q_c)^2/2m$ is the transverse recoil energy. Following [5,6], here we concentrate on the system dynamics for $\bar{\Delta}'_c < 0$, where ω'_0 (i.e., Λ_c) is tunable via Fourier filtering of the intracavity light [86].

Generation of correlated atom pairs via the four-wave mixing terms of $H_{\text{FWM}}^{(1)}$ can be explained by a scattering process illustrated in Fig. 1(d). A photon scattered from the coherent on-axis mode into the initially empty (vacuum) sideband mode a_{\pm} via $a_{\pm}^\dagger a_0 b_{\mp}^\dagger b_0$ can be scattered back into the on-axis mode via $a_0^\dagger a_{\pm} b_{\pm}^\dagger b_0$. This momentum-conserving process creates a correlated pair of indistinguishable atoms with opposite momenta, which can lead to multiparticle entanglement during transient dynamics in a dissipative cavity, as numerically demonstrated in this Letter.

The process can also be described by the atom-only Hamiltonian H_{ad} , for which the photonic modes are adiabatically eliminated (valid for $|\bar{\Delta}_c|, |\bar{\Delta}'_c| \gg \omega_R$) given by $H_{\text{ad}} = H_{\text{pair}} + H'_{\text{ad}}$, where

$$H_{\text{pair}} = -\hbar g_{\text{cav}} b_+^\dagger b_-^\dagger b_0 b_0 + \text{H.c.}, \quad (5)$$

with parameter $g_{\text{cav}} = 2U_0^2\eta^2|\bar{\Delta}'_c|/[(\bar{\Delta}'_c)^2 + \kappa^2](\bar{\Delta}_c^2 + \kappa^2)$ (where $\bar{\Delta}'_c < 0$). In deriving H_{ad} we have neglected $H_{\text{FWM}}^{(2)}$, the influence of photonic sideband creation or annihilation on the coherent field in the on-axis mode, along with the influence of photonic sideband quantum noise on the atomic motion. The relationship of H_B and H_{cav} becomes more apparent now. Indeed, H_{pair} has the form equivalent to H_B , while H'_{ad} describes the energy shifts related to

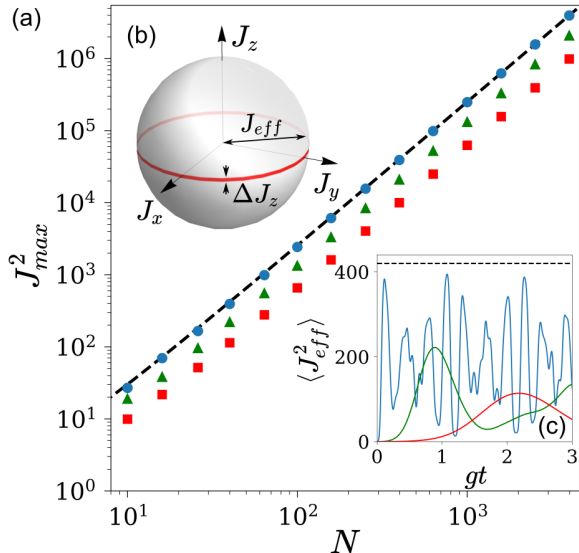


FIG. 2. Populating the sideband Dicke-like states by unitary evolution via H_B and H_{ad} . (a) Maximum $\langle J_{\text{eff}}^2 \rangle$ reached during temporal evolution, denoted by J_{max}^2 (blue dots H_B , red squares H_{ad} at $\eta_{\text{eff}} = 1.6\eta_c$, and green triangles H_{ad} at $\eta_{\text{eff}} = 3\eta_c$) against the total atom number N , with the ideal Dicke state value of $N(N+2)/4$ denoted by the dashed line. (b) The Dicke-squeezed state forms a band around the equator of the Bloch sphere characterized by a large radius $\langle J_{\text{eff}}^2 \rangle = \langle J_x^2 + J_y^2 \rangle$ and a vanishing variance of the “spin” distribution along the z axis, $\langle (\Delta J_z)^2 \rangle$. (c) For unitary evolution with H_B and H_{ad} at $N = 40$, $\langle J_{\text{eff}}^2 \rangle$ (blue line H_B , red line H_{ad} at $\eta_{\text{eff}} = 1.6\eta_c$, green line H_{ad} at $\eta_{\text{eff}} = 3\eta_c$) performs oscillations in time, nearly reaching the limit value of $N(N+2)/4 = 420$ (dashed line) for H_B . For H_B , $g = g_{\text{mod}}$, while for H_{ad} , $g = \omega_R$.

self-organization in the laser-driven system (H'_{ad} and details of the derivation are given in [87]).

Dicke-squeezed states in transverse atomic momentum.—Our aim is to study the phenomenon of Dicke squeezing and the associated multiparticle (many-atom) entanglement for the Hamiltonians H_B , H_{ad} , and H_{cav} . To this end, we define the sideband operators $\delta n = n_+ - n_-$, $\delta N = N_+ - N_-$, along with $J_x = (b_+^\dagger b_- + b_-^\dagger b_+)/2$, $J_y = (b_+^\dagger b_- - b_-^\dagger b_+)/2i$, $J_z = \delta N/2$, which are analogous to Schwinger’s angular momentum operators [101], with $J_{\text{eff}}^2 = J_x^2 + J_y^2$.

Dicke-squeezed states for the transverse momentum sidebands depicted on the Bloch sphere in Fig. 2(b) are characterized by a low $\langle (\Delta J_z)^2 \rangle$, large $\langle J_{\text{eff}}^2 \rangle$, and $\langle J_x \rangle = \langle J_y \rangle = \langle J_z \rangle = 0$ [53,62,63,65,66]. For the two transverse modes, the criterion for Dicke state multiparticle entanglement of identical atoms is given by [66,102]

$$\xi_{\text{gen}}^2 = (N-1) \frac{\langle (\Delta J_z)^2 \rangle}{\langle J_{\text{eff}}^2 \rangle - N/2} < 1, \quad (6)$$

where $N = N_0 + N_+ + N_-$ is the total number of atoms taken as constant in our simulations.

One can easily show that $J_{\text{eff}}^2 = N_+ N_- + (N_+ + N_-)/2$, such that $\langle J_{\text{eff}}^2 \rangle = \langle N_+ N_- \rangle + \langle N_+ + N_- \rangle/2$, where $\langle N_+ N_- \rangle$ is a measure of sideband momentum correlations. For the maximally entangled state, $\langle (\Delta J_z)^2 \rangle = 0$ and $\langle J_{\text{eff}}^2 \rangle = N(N+2)/4$. In the atomic many-body basis, this maximally multiparticle entangled state is the ideal Dicke state, for even N given by $|0\rangle_0 |N/2\rangle_+ |N/2\rangle_-$.

Continuous translational symmetry of H_B and H_{cav} .—Both H_B and H_{cav} are symmetric to continuous translations along the x axis, which leads to $[\delta N, H_B] = 0$ and $[\delta n + \delta N, H_{\text{cav}}] = 0$, where $\langle J_x \rangle = \langle J_y \rangle = \langle J_z \rangle = 0$ for both unitary evolution with H_B and dissipative evolution with H_{cav} [87]. The continuous translational symmetry of H_B and H_{cav} is preserved by the density matrix during temporal evolution. These translationally symmetric self-organized states are analogous to maximally amplitude squeezed photonic states, for which the phase of the electric field is undetermined [103,104].

Unitary evolution under H_B and H_{ad} .—We now discuss the solutions of the Schrödinger equation for H_B and H_{ad} . Because of $[J_z, H_B] = [J_z, H_{\text{ad}}] = 0$, for a system starting in the state $|N\rangle_0 |0\rangle_+ |0\rangle_-$, all moments of J_z will be equal to zero at all t , leading to $\xi_{\text{gen}}^2 = 0$.

The temporal evolution of $\langle J_{\text{eff}}^2 \rangle$ is plotted in Fig. 2(c). The $\langle J_{\text{eff}}^2 \rangle$ initially rises, and then starts to approximately periodically oscillate in time, with the characteristic time-scale $\tau \sim 2\pi/(Ng_{\text{mod}})$ for H_B and $\tau \sim 2\pi/(Ng_{\text{cav}}) = 4\pi\eta_c^2/(\omega_R\eta_{\text{eff}}^2)$ for H_{ad} [105]. For H_B , the atoms scatter in and out of the transverse sidebands by absorbing and emitting energy quanta from and to the driving magnetic field, while for H_{ad} one observes sloshing dynamics (see below). The value of $\langle J_{\text{eff}}^2 \rangle$ oscillates with a large amplitude, nearly reaching 0 at its trough and $N(N+2)/4$ for H_B at its peak.

The available Hilbert space is for this initial condition significantly reduced, as states keep zero transverse atomic momentum during unitary evolution, allowing for simulations with relatively large N . Plotting the highest J_{eff}^2 reached during temporal evolution for H_B and H_{ad} , denoted by J_{max}^2 , versus N , reveals a rise parallel to the $N(N+2)/4$ line over nearly 3 orders of magnitude, up to the maximum atom number tractable by the computational resources available; see Fig. 2(a).

The N^2 scaling of J_{max}^2 observed for large N during unitary evolution demonstrates the high efficiency of H_B and H_{ad} in generating momentum entangled atoms, which echoes the efficiency of optical parametric amplifiers in generating photonic entanglement [77].

Dissipative dynamics under H_{cav} and H_{ad} .—We first look at the full photon-atom dynamics for both the coherent unitary evolution and for including the cavity photon decay in the Lindblad master equation. Because of conservation

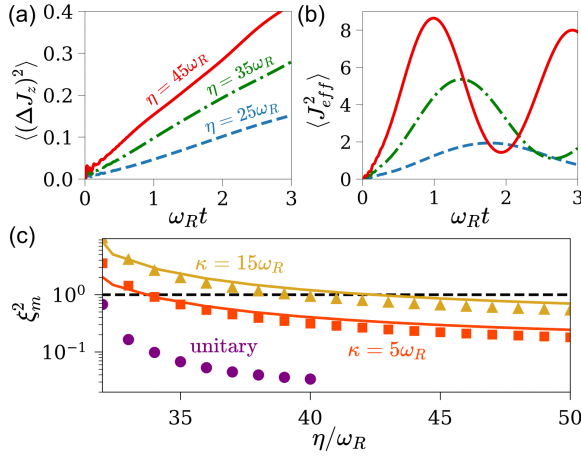


FIG. 3. Generating multiparticle entanglement in the Dicke-like states via transverse self-organization for the full system Hamiltonian H_{cav} . The dissipative dynamical evolution of (a) $\langle (\Delta J_z)^2 \rangle$, (b) $\langle J_{\text{eff}}^2 \rangle$ for η values of $25\omega_R$ (blue, dashed), $35\omega_R$ (green, dot-dashed), and $45\omega_R$ (red, solid). (c) The η scan of ξ_m^2 given by the lowest ξ_{gen}^2 reached during temporal evolution, for the unitary case (purple, dots), and $\kappa = 5\omega_R$ (red, squares), $\kappa = 15\omega_R$ (yellow, triangles). Crossing of the dashed line ($\xi_{\text{gen}}^2 = 1$) indicates the existence of many-particle entanglement [102]. Solid lines in (c) are results for the H_{ad} model with $\eta_{\text{eff}} = 0.56\eta$. Simulation parameters: (a), (b) $(\bar{\Delta}_c, \bar{\Delta}'_c, U_0, \kappa) = (110, -45, 10, 5)\omega_R$, and (c) $(\bar{\Delta}_c, \bar{\Delta}'_c, U_0) = (110, -45, 10)\omega_R$, with (a)–(c) $N = 8$.

of momentum in the combined photon-atom four-wave mixing, we have $[\delta n + \delta N, H_{\text{cav}}] = 0$, but $[J_z, H_{\text{cav}}] \neq 0$. The Hilbert space in this problem is considerably larger than for H_B , which limits the tractable atom number to $N = 8$ for the calculations of full quantum dynamics. Parameter values for this case are taken such that maximal Dicke squeezing is observed, and experimentally accessible parameters are discussed in [87].

Because of $[\delta n + \delta N, H_{\text{cav}}] = 0$, the variance of $2J_z$ is equal to the variance of δn for the unitarily evolving system. This indicates that a reduction of ξ_{gen}^2 will benefit from lower δn variances, which in general occur when $\langle n_0 \rangle$ and $\langle n_{\pm} \rangle$ are lower, e.g., at larger $|\bar{\Delta}_c|$, $|\bar{\Delta}'_c|$, as long as $\langle J_{\text{eff}}^2 \rangle$ is large.

In Figs. 3(a) and 3(b), we plot the temporal evolution of the relevant atomic observables for varying the pump strength η in the case with dissipation of photons out of the cavity. For the dissipative case, the equality of δN and δn variances no longer holds, and the dissipation of photons out of the cavity makes $\langle (\Delta J_z)^2 \rangle$ increase almost linearly with time, with the slope increasing with the pump amplitude η . This indicates that there is still correlation between δN and δn even in the dissipative case; i.e., the low δn variances obtained for lower $\langle n_{\pm} \rangle$ will lead to lower δN variances.

The $\langle J_{\text{eff}}^2 \rangle$ initially increases and oscillates in time, again indicating sloshing dynamics, with continuous oscillations between the bunched and nearly homogeneous structures in the self-ordered atomic lattice (see also [6,106]). Increasing

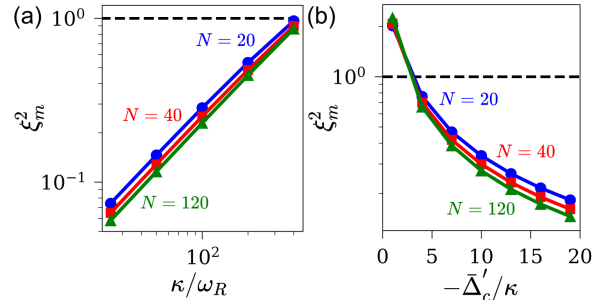


FIG. 4. Entanglement generation for a dissipative cavity with adiabatically eliminated photonic fields described by the Lindblad master equation with H_{ad} and decay rate γ (see text). (a) Cavity decay rate κ scan of ξ_m^2 (see text) for fixed $(\bar{\Delta}_c, \bar{\Delta}'_c) = (1400, -1200)\omega_R$, and $N = 20$ (blue dots), $N = 40$ (red squares), and $N = 120$ (green triangles). (b) Sideband detuning $\bar{\Delta}'_c$ scan of ξ_m^2 for N values as in (a), and fixed $\kappa = 3 \times 10^4\omega_R$, with $\bar{\Delta}_c = |\bar{\Delta}'_c| + 4\kappa$ for each point. The dashed line indicates $\xi_{\text{gen}}^2 = 1$. Solid lines are guide to the eyes. Simulation parameters: $U_0 = 10^{-3}\omega_R$, $\eta_{\text{eff}} = 1.6\eta_c$.

the pump η , both the growth rate and maximum value of $\langle J_{\text{eff}}^2 \rangle$ are increased. The growth rate of $\langle J_{\text{eff}}^2 \rangle$ increases faster with distance to the threshold than the growth rate of $\langle (\Delta J_z)^2 \rangle$, which, from Eq. (6), leads to a decrease in ξ_{gen}^2 for larger η . Increasing the η values several times above the semiclassically calculated threshold $\eta_c = [-\omega_R(\bar{\Delta}_c^2 + \kappa^2)(\bar{\Delta}'_c^2 + \kappa^2)/(4NU_0^2\bar{\Delta}'_c)]^{1/2} \approx 13\omega_R$ [87], the ξ_m^2 given by the lowest ξ_{gen}^2 attained during temporal evolution reaches values of $\xi_m^2 = 0.03$ for the unitary and $\xi_m^2 = 0.18$ for the dissipative case; see Fig. 3(c). We have also performed simulations of dissipative dynamics with adiabatically eliminated photonic modes described by a Lindblad master equation with H_{ad} and decay rate $\gamma = U_0^2\eta_{\text{eff}}^2\kappa/[(\bar{\Delta}'_c^2 + \kappa^2)(\bar{\Delta}_c^2 + \kappa^2)]$. The H_{ad} calculations with $\eta_{\text{eff}} = 0.56\eta$ reproduce well the squeezing for the full model, as shown in Fig. 3(c). The rescaling of η_{eff} with respect to η is a consequence of neglecting the nonlinear saturation and on-axis mode depletion terms in deriving H_{ad} [87].

For higher N calculations reachable with the H_{ad} model, the ξ_m^2 again decreases for decreasing the decay rate κ at fixed detunings $\bar{\Delta}_c$, $\bar{\Delta}'_c$, and η_{eff}/η_c [see Fig. 4(a)], which is a consequence of increasing the ratio $-g_{\text{cav}}/\gamma = 2|\bar{\Delta}'_c|/\kappa$, leading toward coherent cavity dynamics, similarly to the single-mode cavity case [54,105]. The parameters $\bar{\Delta}'_c/\kappa$ and η_{eff}/η_c completely determine the open system dynamics for H_{ad} with N atoms. Intriguingly, significant squeezing can be achieved in this model for large $-\bar{\Delta}'_c/\kappa$ even with “bad cavity” parameters. Indeed, using the finesse $F = 250$ and a free spectral range of $\text{FSR} = 1.5$ GHz, with $\kappa/(2\pi) = \text{FSR}/(2F) = 3$ MHz and $\omega_R = 2\pi \times 0.1$ kHz, we demonstrate in Fig. 4(b) that nearly 10 dB squeezing is attainable for $N = 120$ atoms.

Conclusion.—Momentum entanglement of ultracold atoms holds great potential for enhancing matter wave interferometry [107]. We have theoretically and numerically explored two methods for producing momentum multiparticle entangled (Dicke-squeezed) states of atoms with one internal ground state (spin-0) by nonlinear self-organization in driven systems. For H_B the drive is an oscillating magnetic field, and the method is based on the experiment of Ref. [31]. A novel model H_{cav} based on laser driving of a two-level optical transition of a BEC with ring cavity feedback is also developed and explored. Although entanglement occurs here in the transient dynamical regime, it can readily be shown that switching off the driving field at the moment of optimal squeezing preserves the momentum distribution and thus also the entanglement for a longer time [87]. The three-mode picture, for which the higher-order momentum sideband population is considered negligible, can prove incomplete when scattering to higher-order modes is strong, which is explored in [87].

Experimental determination of $\langle(\Delta J_z)^2\rangle$ and $\langle J_{\text{eff}}^2\rangle$ relies on assessing the momentum correlations via $\langle N_+N_-\rangle$. Absorption imaging of the atomic momentum distribution with a highly efficient camera can be used to measure N_+N_- for each experimental realization, and $\langle N_+N_-\rangle$ can then be determined by taking the average for many realizations. Alternative ways of measuring atomic momentum correlations are given, e.g., in [63,108]. Note that Dicke-squeezing generation described in this Letter is based on continuous symmetry of H_B and H_{cav} , which is also present for some prominent recent models describing self-organization of ultracold atoms [17,23].

Moreover, since the calculations show significant momentum squeezing is available even for low finesse values, a relatively simple setup with a nearly degenerate cavity external to the vacuum chamber may be sufficient to realize it experimentally. Another highly intriguing prospect is the possibility of generating correlations in thermal and ultracold atomic degrees of freedom in a single mirror feedback setup [12,26,109–113] or using counterpropagating beams [9,114,115].

We thank Tobias Donner, Oliver Diekmann, Helmut Ritsch, Berislav Buča, Paul Griffin, and Onur Hosten for helpful discussions. The work of I. K. was funded by the Austrian Science Fund Lise Meitner Postdoctoral Fellowship M3011 and an ESQ Discovery grant from the Austrian Academy of Sciences. The dynamical evolution equations were solved numerically by using the open-source framework QUANTUMOPTICS.JL [116]. The computational results presented here have been achieved using the Vienna Scientific Cluster.

- [3] P. Domokos and H. Ritsch, *Phys. Rev. Lett.* **89**, 253003 (2002).
- [4] A. T. Black, H. W. Chan, and V. Vuletić, *Phys. Rev. Lett.* **91**, 203001 (2003).
- [5] K. Baumann, C. Guerlin, F. Brennecke, and T. Esslinger, *Nature (London)* **464**, 1301 (2010).
- [6] D. Nagy, G. Konya, G. Szirmai, and P. Domokos, *Phys. Rev. Lett.* **104**, 130401 (2010).
- [7] S. Gopalakrishnan, B. L. Lev, and P. M. Goldbart, *Nat. Phys.* **5**, 845 (2009).
- [8] S. Gopalakrishnan, B. L. Lev, and P. M. Goldbart, *Phys. Rev. A* **82**, 043612 (2010).
- [9] J. A. Greenberg, B. L. Schmittberger, and D. J. Gauthier, *Opt. Express* **19**, 22535 (2011).
- [10] E. Tesio, Theory of self-organisation in cold atoms, Ph.D. thesis, University of Strathclyde, 2014, [10.48730/mk5nbz40](https://doi.org/10.48730/mk5nbz40).
- [11] E. Tesio, G. R. M. Robb, T. Ackemann, W. J. Firth, and G.-L. Oppo, *Phys. Rev. Lett.* **112**, 043901 (2014).
- [12] G. Labeyrie, E. Tesio, P. M. Gomes, G.-L. Oppo, W. J. Firth, G. R. M. Robb, A. S. Arnold, R. Kaiser, and T. Ackemann, *Nat. Photonics* **8**, 321 (2014).
- [13] G. R. M. Robb, E. Tesio, G.-L. Oppo, W. J. Firth, T. Ackemann, and R. Bonifacio, *Phys. Rev. Lett.* **114**, 173903 (2015).
- [14] B. L. Schmittberger and D. J. Gauthier, *New J. Phys.* **18**, 103021 (2016).
- [15] S. Ostermann, F. Piazza, and H. Ritsch, *Phys. Rev. X* **6**, 021026 (2016).
- [16] K. E. Ballantine, B. L. Lev, and J. Keeling, *Phys. Rev. Lett.* **118**, 045302 (2017).
- [17] J. Léonard, A. Morales, P. Zupancic, T. Esslinger, and T. Donner, *Nature (London)* **543**, 87 (2017).
- [18] A. J. Kollár, A. T. Papageorge, V. D. Vaidya, Y. Guo, J. Keeling, and B. L. Lev, *Nat. Commun.* **8**, 14386 (2017).
- [19] Y.-C. Zhang, V. Walther, and T. Pohl, *Phys. Rev. Lett.* **121**, 073604 (2018).
- [20] V. D. Vaidya, Y. Guo, R. M. Kroese, K. E. Ballantine, A. J. Kollar, J. Keeling, and B. L. Lev, *Phys. Rev. X* **8**, 011002 (2018).
- [21] Y. Guo, R. M. Kroese, V. D. Vaidya, J. Keeling, and B. L. Lev, *Phys. Rev. Lett.* **122**, 193601 (2019).
- [22] Y. Guo, V. D. Vaidya, R. M. Kroese, R. A. Lunney, B. L. Lev, and J. Keeling, *Phys. Rev. A* **99**, 053818 (2019).
- [23] S. C. Schuster, P. Wolf, S. Ostermann, S. Slama, and C. Zimmermann, *Phys. Rev. Lett.* **124**, 143602 (2020).
- [24] G. Baio, G. R. M. Robb, A. M. Yao, G.-L. Oppo, and T. Ackemann, *Phys. Rev. Lett.* **126**, 203201 (2021).
- [25] Y. Guo, R. M. Kroese, B. P. Marsh, S. Gopalakrishnan, J. Keeling, and B. L. Lev, *Nature (London)* **599**, 211 (2021).
- [26] T. Ackemann, G. Labeyrie, G. Baio, I. Krešić, J. G. M. Walker, A. Costa Boquete, P. Griffin, W. J. Firth, R. Kaiser, G.-L. Oppo, and G. R. M. Robb, *Atoms* **9**, 35 (2021).
- [27] P. Engels, C. Atherton, and M. A. Hoefer, *Phys. Rev. Lett.* **98**, 095301 (2007).
- [28] J. Kronjäger, C. Becker, P. Soltan-Panahi, K. Bongs, and K. Sengstock, *Phys. Rev. Lett.* **105**, 090402 (2010).
- [29] S. E. Pollack, D. Dries, R. G. Hulet, K. M. F. Magalhães, E. A. L. Henn, E. R. F. Ramos, M. A. Caracanhas, and V. S. Bagnato, *Phys. Rev. A* **81**, 053627 (2010).

*ivor.kresic@tuwien.ac.at

- [1] H. Ritsch, P. Domokos, F. Brennecke, and T. Esslinger, *Rev. Mod. Phys.* **85**, 553 (2013).
- [2] F. Mivehvar, F. Piazza, T. Donner, and H. Ritsch, *Adv. Phys.* **70**, 1 (2021).

- [30] J. H. V. Nguyen, M. C. Tsatsos, D. Luo, A. U. J. Lode, G. D. Telles, V. S. Bagnato, and R. G. Hulet, *Phys. Rev. X* **9**, 011052 (2019).
- [31] Z. Zhang, K.-X. Yao, L. Feng, J. Hu, and C. Chin, *Nat. Phys.* **16**, 652 (2020).
- [32] L. A. Lugiato and F. Castelli, *Phys. Rev. Lett.* **68**, 3284 (1992).
- [33] G. Grynberg and L. A. Lugiato, *Opt. Commun.* **101**, 69 (1993).
- [34] A. Gatti and S. Mancini, *Phys. Rev. A* **65**, 013816 (2001).
- [35] M. M. Cola, M. G. A. Paris, and N. Piovella, *Phys. Rev. A* **70**, 043809 (2004).
- [36] I. B. Mekhov, C. Maschler, and H. Ritsch, *Nat. Phys.* **3**, 319 (2007).
- [37] D. Nagy, P. Domokos, A. Vukics, and H. Ritsch, *Eur. Phys. J. D* **55**, 659 (2009).
- [38] D. Nagy, G. Szirmai, and P. Domokos, *Phys. Rev. A* **84**, 043637 (2011).
- [39] T. J. Elliott, W. Kozlowski, S. F. Caballero-Benitez, and I. B. Mekhov, *Phys. Rev. Lett.* **114**, 113604 (2015).
- [40] S. Ostermann, W. Niedenzu, and H. Ritsch, *Phys. Rev. Lett.* **124**, 033601 (2020).
- [41] D. A. Ivanov, T. Y. Ivanova, S. F. Caballero-Benitez, and I. B. Mekhov, *Phys. Rev. Lett.* **124**, 010603 (2020).
- [42] V. Giovannetti, S. Lloyd, and L. Maccone, *Phys. Rev. Lett.* **96**, 010401 (2006).
- [43] A. A. Clerk, M. H. Devoret, S. M. Girvin, F. Marquardt, and R. J. Schoelkopf, *Rev. Mod. Phys.* **82**, 1155 (2010).
- [44] L.-M. Duan, A. Sørensen, J. I. Cirac, and P. Zoller, *Phys. Rev. Lett.* **85**, 3991 (2000).
- [45] H. Pu and P. Meystre, *Phys. Rev. Lett.* **85**, 3987 (2000).
- [46] A. Sørensen, L.-M. Duan, J. I. Cirac, and P. Zoller, *Nature (London)* **409**, 63 (2001).
- [47] C. Gross, T. Zibold, E. Nicklas, J. Estève, and M. K. Oberthaler, *Nature (London)* **464**, 1165 (2010).
- [48] I. D. Leroux, M. H. Schleier-Smith, and V. Vuletic, *Phys. Rev. Lett.* **104**, 073602 (2010).
- [49] M. H. Schleier-Smith, I. D. Leroux, and V. Vuletic, *Phys. Rev. A* **81**, 021804(R) (2010).
- [50] C. Gross, *J. Phys. B* **45**, 103001 (2012).
- [51] O. Hosten, N. J. Engelsen, R. Krishnakumar, and M. A. Kasevich, *Nature (London)* **529**, 505 (2016).
- [52] X.-Y. Luo, Y.-Q. Zou, L.-N. Wu, Q. Liu, M.-F. Han, M. K. Tey, and L. You, *Science* **355**, 620 (2017).
- [53] L. Pezze, A. Smerzi, M. K. Oberthaler, R. Schmied, and P. Treutlein, *Rev. Mod. Phys.* **90**, 035005 (2018).
- [54] E. J. Davis, G. Bentsen, L. Homeier, T. Li, and M. H. Schleier-Smith, *Phys. Rev. Lett.* **122**, 010405 (2019).
- [55] A. Chu, P. He, J. K. Thompson, and A. M. Rey, *Phys. Rev. Lett.* **127**, 210401 (2021).
- [56] L. Salvi, N. Poli, V. Vuletić, and G. M. Tino, *Phys. Rev. Lett.* **120**, 033601 (2018).
- [57] K. Gietka, F. Mivehvar, and H. Ritsch, *Phys. Rev. Lett.* **122**, 190801 (2019).
- [58] A. Shankar, L. Salvi, M. L. Chiofalo, N. Poli, and M. J. Holland, *Quantum Sci. Technol.* **4**, 045010 (2019).
- [59] F. Anders, A. Idel, P. Feldmann, D. Bondarenko, S. Loriani, K. Lange, J. Peise, M. Gersemann, B. Meyer-Hoppe, S. Abend, N. Gaaloul, C. Schubert, D. SchlipPERT, L. Santos, E. Rasel, and C. Klemp, *Phys. Rev. Lett.* **127**, 140402 (2021).
- [60] G. P. Greve, C. Luo, B. Wu, and J. K. Thompson, *Nature (London)* **610**, 472 (2022).
- [61] J. A. Dunningham, K. Burnett, and S. M. Barnett, *Phys. Rev. Lett.* **89**, 150401 (2002).
- [62] B. Lücke, M. Scherer, J. Kruse, L. Pezze, F. Deuretzbacher, P. Hyllus, O. Topic, J. Peise, W. Ertmer, J. Arlt, L. Santos, A. Smerzi, and C. Klemp, *Science* **334**, 773 (2011).
- [63] R. Bücker, J. Grond, S. Manz, T. Berrada, T. Betz, C. Koller, U. Hohenester, T. Schumm, A. Perrin, and J. Schmiedmayer, *Nat. Phys.* **7**, 608 (2011).
- [64] L.-M. Duan, *Phys. Rev. Lett.* **107**, 180502 (2011).
- [65] Z. Zhang and L. M. Duan, *New J. Phys.* **16**, 103037 (2014).
- [66] B. Lücke, J. Peise, G. Vitagliano, J. Arlt, L. Santos, G. Tóth, and C. Klemp, *Phys. Rev. Lett.* **112**, 155304 (2014).
- [67] L. Deng, E. W. Hagley, J. Wen, M. Trippenbach, Y. Band, P. S. Julienne, J. Simsarian, K. Helmerson, S. Rolston, and W. D. Phillips, *Nature (London)* **398**, 218 (1999).
- [68] J. M. Vogels, K. Xu, and W. Ketterle, *Phys. Rev. Lett.* **89**, 020401 (2002).
- [69] N. Gemelke, E. Sarajlic, Y. Bidel, S. Hong, and S. Chu, *Phys. Rev. Lett.* **95**, 170404 (2005).
- [70] G. K. Campbell, J. Mun, M. Boyd, E. W. Streed, W. Ketterle, and D. E. Pritchard, *Phys. Rev. Lett.* **96**, 020406 (2006).
- [71] A. Perrin, H. Chang, V. Krachmalnicoff, M. Schellekens, D. Boiron, A. Aspect, and C. I. Westbrook, *Phys. Rev. Lett.* **99**, 150405 (2007).
- [72] R. G. Dall, L. J. Byron, A. G. Truscott, G. R. Dennis, M. T. Johnsson, and J. J. Hope, *Phys. Rev. A* **79**, 011601(R) (2009).
- [73] J.-C. Jaskula, M. Bonneau, G. B. Partridge, V. Krachmalnicoff, P. Deuar, K. V. Kheruntsyan, A. Aspect, D. Boiron, and C. I. Westbrook, *Phys. Rev. Lett.* **105**, 190402 (2010).
- [74] W. H. Louisell, A. Yariv, and A. E. Siegman, *Phys. Rev.* **124**, 1646 (1961).
- [75] C. M. Caves and B. L. Schumaker, *Phys. Rev. A* **31**, 3068 (1985).
- [76] B. Yurke, S. L. McCall, and J. R. Klauder, *Phys. Rev. A* **33**, 4033 (1986).
- [77] R. Schnabel, *Phys. Rep.* **684**, 1 (2017).
- [78] D. Linnemann, H. Strobel, W. Muessel, J. Schulz, R. J. Lewis-Swan, K. V. Kheruntsyan, and M. K. Oberthaler, *Phys. Rev. Lett.* **117**, 013001 (2016).
- [79] S. S. Szigeti, R. J. Lewis-Swan, and S. A. Haine, *Phys. Rev. Lett.* **118**, 150401 (2017).
- [80] L. A. Lugiato and R. Lefever, *Phys. Rev. Lett.* **58**, 2209 (1987).
- [81] L. A. Lugiato and C. Oldano, *Phys. Rev. A* **37**, 3896 (1988).
- [82] E. Tesio, G. R. M. Robb, T. Ackemann, W. J. Firth, and G.-L. Oppo, *Phys. Rev. A* **86**, 031801(R) (2012).
- [83] T. Ackemann, S. Barland, J. R. Tredicce, M. Cara, S. Balle, R. Jäger, M. Grabherr, M. Miller, and K. J. Ebeling, *Opt. Lett.* **25**, 814 (2000).

- [84] A. Esteban-Martín, J. García, E. Roldán, V. B. Taranenko, G. J. de Valcárcel, and C. O. Weiss, *Phys. Rev. A* **69**, 033816 (2004).
- [85] A. Esteban-Martín, V. B. Taranenko, J. García, G. J. de Valcárcel, and E. Roldán, *Phys. Rev. Lett.* **94**, 223903 (2005).
- [86] S. J. Jensen, M. Schwab, and C. Denz, *Phys. Rev. Lett.* **81**, 1614 (1998).
- [87] See Supplemental Material at <http://link.aps.org/supplemental/10.1103/PhysRevLett.131.163602> for additional details on the derivations of the Hamiltonians, mean field calculations, continuous translational symmetry considerations, and potential experimental implementation, including Refs. [88–100].
- [88] C. Maschler, I. B. Mekhov, and H. Ritsch, *Eur. Phys. J. D* **46**, 545 (2008).
- [89] V. Torggler and H. Ritsch, *Optica* **1**, 336 (2014).
- [90] H.-P. Breuer and F. Petruccione, *The Theory of Open Quantum Systems* (Oxford University Press, New York, 2002).
- [91] V. V. Albert and L. Jiang, *Phys. Rev. A* **89**, 022118 (2014).
- [92] J. Preskill, *Cal. Inst. Technol.* **16**, 1 (1998).
- [93] P. Domokos and H. Ritsch, *J. Opt. Soc. Am. B* **20**, 1098 (2003).
- [94] A. J. Kollár, A. T. Papageorge, K. Baumann, M. A. Armen, and B. L. Lev, *New J. Phys.* **17**, 043012 (2015).
- [95] J. H. V. Nguyen, D. Luo, and R. G. Hulet, *Science* **356**, 422 (2017).
- [96] Y. Slobodkin, G. Weinberg, H. Hörner, K. Pichler, S. Rotter, and O. Katz, *Science* **377**, 995 (2022).
- [97] A. Dombi, T. Clark, F. Williams, F. Jessen, J. Fortágh, D. Nagy, A. Vukics, and P. Domokos, *New J. Phys.* **23**, 083036 (2021).
- [98] C. W. Gardiner and M. J. Collett, *Phys. Rev. A* **31**, 3761 (1985).
- [99] K. W. Murch, K. L. Moore, S. Gupta, and D. M. Stamper-Kurn, *Nat. Phys.* **4**, 561 (2008).
- [100] B. W. Shore and P. L. Knight, *J. Mod. Opt.* **40**, 1195 (1993).
- [101] J. Schwinger, On angular momentum, U.S. Atomic Energy Commission Technical Report No. NYO-3071, 1952 [Reprinted in *Quantum Theory of Angular Momentum*, edited by L. Biedenharn and H. Van Dam (Academic Press, New York, 1965)].
- [102] G. Tóth, C. Knapp, O. Gühne, and H. J. Briegel, *Phys. Rev. A* **79**, 042334 (2009).
- [103] C. M. Caves, *Phys. Rev. D* **26**, 1817 (1982).
- [104] D. F. Walls, *Nature (London)* **306**, 141 (1983).
- [105] F. Finger, R. Rosa-Medina, N. Reiter, P. Christodoulou, T. Donner, and T. Esslinger, [arXiv:2303.11326](https://arxiv.org/abs/2303.11326).
- [106] E. Tesio, G. R. M. Robb, G.-L. Oppo, P. M. Gomes, T. Ackemann, G. Labeyrie, R. Kaiser, and W. J. Firth, *Phil. Trans. R. Soc. A* **372**, 20140002 (2014).
- [107] S. S. Szigeti, O. Hosten, and S. A. Haine, *Appl. Phys. Lett.* **118**, 140501 (2021).
- [108] F. Borselli, M. Maiwöger, T. Zhang, P. Haslinger, V. Mukherjee, A. Negretti, S. Montangero, T. Calarco, I. Mazets, M. Bonneau, and J. Schmiedmayer, *Phys. Rev. Lett.* **126**, 083603 (2021).
- [109] G. D’Alessandro and W. J. Firth, *Phys. Rev. Lett.* **66**, 2597 (1991).
- [110] I. Krešić, G. Labeyrie, G. R. M. Robb, G.-L. Oppo, P. M. Gomes, P. Griffin, R. Kaiser, and T. Ackemann, *Commun. Phys.* **1**, 33 (2018).
- [111] G. Labeyrie, I. Krešić, G. R. M. Robb, G.-L. Oppo, R. Kaiser, and T. Ackemann, *Optica* **5**, 1322 (2018).
- [112] I. Krešić, G. R. M. Robb, G. Labeyrie, R. Kaiser, and T. Ackemann, *Phys. Rev. A* **99**, 053851 (2019).
- [113] G. Labeyrie, J. G. M. Walker, G. R. M. Robb, R. Kaiser, and T. Ackemann, *Phys. Rev. A* **105**, 023505 (2022).
- [114] A. Yariv and D. M. Pepper, *Opt. Lett.* **1**, 16 (1977).
- [115] W. J. Firth, I. Krešić, G. Labeyrie, A. Camara, and T. Ackemann, *Phys. Rev. A* **96**, 053806 (2017).
- [116] S. Krämer, D. Plankensteiner, L. Ostermann, and H. Ritsch, *Comput. Phys. Commun.* **227**, 109 (2018).